Special issue on Recent advances in photomodulation in higher plants, algae, and bryophytes

Variation in leaf mesophyll anatomy of fern species imposes significant effects on leaf gas exchange, light capture, and leaf hydraulic conductance

S. FUJII[*], K. NISHIDA[*], T.K. AKITSU[**] (iD), A. KUME[***] (iD), and Y.T. HANBA[*,+] (iD)

Kyoto Institute of Technology, Matsugasaki, Sakyo-ku, 606-8585 Kyoto, Japan[*]
Earth Observation Research Center, Japan Aerospace Exploration Agency, 2-1-1 Sengen, 305-8505 Tsukuba, Japan[**]
Faculty of Agriculture, Kyushu University, 744 Motooka, Nishi-ku, 819-0395 Fukuoka, Japan[***]

Abstract

The mesophyll anatomical traits are essential factors for efficient light capture, CO_2 diffusion, and hydraulics in leaves. At the same time, leaf hydraulics are governed by the xylem anatomical traits. Thus, simultaneous analyses of the mesophyll and xylem anatomy will clarify the links among light capture, CO_2 capture, and water use. However, such simultaneous analyses have been scarcely performed, particularly on non-seed plants. Using seven fern species, we first showed that fern species with a large mesophyll thickness had a high photosynthetic rate related to high light capture, high drought tolerance, and low leaf hydraulic conductance. The chloroplast surface area (S_c) per mesophyll thickness significantly decreased with an increase in mesophyll thickness, which may increase light diffusion and absorption efficiency in each chloroplast. The photosynthetic rate per S_c was almost constant with mesophyll thickness, which suggests that ferns enhance their light capture ability *via* the regulation of chloroplast density.

Introduction

Leaf mesophyll anatomy is one of the key factors determining leaf photosynthesis *via* CO_2 diffusion and light interception (Ren *et al.* 2019). Leaves with a thick mesophyll, such as the sun leaves in angiosperms, have a high rate of photosynthesis on a leaf-area-basis (Hanba *et al.* 1999, Lambers and Oliveira 2019). Such a high photosynthetic rate is strongly affected by the enhanced CO_2 diffusion through many chloroplasts that involve a large chloroplast surface area for CO_2 diffusion, S_c/S (Hanba *et al.* 1999, 2002; Oguchi *et al.* 2005, Tosens *et al.* 2012, Fini *et al.* 2016). The leaf anatomy is well-designed to maximize light absorption. That is, the leaves

Highlights

- Simultaneous analyses of the mesophyll and xylem anatomy were performed for seven fern species
- Ferns coordinate leaf gas exchange, light capture, and leaf hydraulics *via* mesophyll thickness
- The photosynthetic rate per chloroplast in ferns higher than that in bryophytes was shown for the first time

with a thick mesophyll in angiosperms, such as the sun leaves grown under a strong light environment, have more elongated palisade cells that enhance light transmission in the leaves and spread the light through the depth of the leaf (Cui *et al.* 1991, Kume 2017). In the thick, multi-layered palisade tissue in angiosperms, the absorbed photons in each chloroplast reduce as the thickness increases (Kume 2017). In other words, reducing the thickness leads to an increase in the absorbed photons in each chloroplast. Even in leaves grown under a low light environment, reducing mesophyll thickness is preferable for efficient light capture (Matos *et al.* 2009).

It makes sense that plants with a large leaf mesophyll thickness have higher leaf hydraulic conductance as a large mesophyll thickness is related to a high photosynthetic rate and high stomatal conductance, which results in great evaporative demand. However, there is controversy about how leaf hydraulic conductance relates to mesophyll thickness (Sack *et al.* 2015). We found the opposite dependence has also been reported (Aasamaa *et al.* 2001, Brodribb *et al.* 2007). Accordingly, the dependence might vary with the mesophyll anatomy, xylem anatomy, and leaf water status (Sack *et al.* 2013). On the other hand, leaf hydraulic conductance is strongly related to xylem anatomical traits such as the size of the water transport tissues, *e.g.*, a wider diameter of a vessel or tracheid results in greater leaf hydraulic conductance (Zanne *et al.* 2010). Thus, simultaneous analyses of the mesophyll anatomy and xylem anatomy would contribute greatly to clarifying the links among CO_2 capture, light capture, and leaf hydraulics. However, such simultaneous analyses have been scarcely performed, particularly on non-seed plants such as ferns and bryophytes. For the early land plants, which are the common ancestors of ferns and bryophytes, light and water use by photosynthetic organs are two important adaptive traits. Significant morphological evolution may have occurred in ferns and bryophytes for the efficient use of light and water. To evaluate such an evolutionary process, it would be useful to evaluate the functions of various morphological properties of leaves related to light and water use at different diversification ages.

In the first experiment in the present study, we performed a growth experiment of the seven fern species with diverse mesophyll and xylem anatomy. Our purpose was to clarify the interrelationships among CO_2 capture, light capture, and leaf hydraulics in fern species *via* analyses of the mesophyll and xylem anatomy. Ferns are suitable for this analysis because fern species have similar leaf structures of serrated flat leaves but have large interspecific variations in the mesophyll anatomy, xylem anatomy, photosynthesis, and leaf hydraulic conductance. The Selaginellaceae species in lycophytes have only one or two layers of mesophyll cells with a very low photosynthetic rate (Carriquí *et al.* 2019), while *Dryopteris erythrosora* in the Dryopteridaceae family has over three layers of mesophyll cells (Tosens *et al.* 2016), enabling a high photosynthetic rate. A wide range of variations in hydraulic conductance and tracheid diameter has been

reported for 16 fern species from ten families (Pittermann *et al.* 2011).

Second, we measured the light absorptance of two selected fern species using a spectroradiometer to obtain the direct effect of the mesophyll anatomy on the light capture of the leaves. Finally, to highlight the features of the ferns concerning the effect of mesophyll anatomy on CO_2 capture and light capture, we compared the related data between ferns and bryophytes using data from previous studies. We tested the following hypotheses:

(*1*) Fern species with a thick mesophyll have a high photosynthetic rate, largely due to enhanced CO_2 diffusion caused by anatomical traits such as a larger chloroplast surface area facing the intercellular airspace on an area-basis (S_c/S).

(*2*) Ferns with a large mesophyll thickness have a large ability to capture light and high hydraulic conductivity.

(*3*) Ferns have a higher photosynthetic rate, more efficient light capture, and CO_2 diffusion compared to bryophytes.

Materials and methods

Growth experiment for the seven fern species: We used fern species that are distributed in the temperate region in Japan, including species of various orders and evolutionary ages (Table 1, Fig. 1). The seven species were used for the detailed analyses of leaf mesophyll anatomy, xylem anatomy, leaf gas exchange, and leaf hydraulic conductance, in which the growth experiments were performed in June–October 2014 and 2015. An additional growth experiment was performed in 2019 using two other species, *Marsilea quadrifolia* and *Pyrrosia lingua*, to clarify the effect of mesophyll anatomy on the absorptance of radiation. These nine fern plants were purchased from commercial nurseries and grown in glasshouses at the campus of the Kyoto Institute of Technology in Kyoto City (35°03'N, 135°47'E).

In the experiments in 2014 and 2015, the seven fern species were transplanted to 3.3-L Wagner pots filled with cultivated soil containing fertilizer (Fig. 1*B*). We used the emerging leaves of plants grown for at least six months in the glasshouse for the following measurements. The plants were watered daily and fertilized with 200 mL of 1/500 *Hyponex* solution (*Hyponex Japan*, Osaka, Japan) once a week. In the glasshouse, the daily mean temperature, daily mean relative humidity, and maximum daily PPFD were 21–30°C, 43–82%, and 300–600 µmol m^{-2} s^{-1}, respectively. For the experiment in 2019, we cultivated two fern species in another glasshouse where the temperature was controlled at 25°C. Healthy, fully expanded mature leaves were used for the following measurements.

Leaf gas exchange: Six attached leaves from each of the seven fern species were used for the measurements (*n* = 6). Healthy, fully expanded mature leaves were used. Leaf photosynthesis was measured using *Li-6400XT* (*Li-Cor*, Lincoln, NE, USA) from 10:00 to 18:00 h in a day. The leaf temperature was set at 25°C and the vapor

Table 1. Descriptions of the seven fern species used for the detailed anatomical and physiological measurements and the two fern species used for the light absorptance measurements. Order or suborder, family, species name, epiphyte or terrestrial, light and water requirement, and diversification age of the family are shown. The mean evolutionary age of the family was estimated from the literature (Pryer et al. 2004, Schuettpelz and Pryer 2009, Testo et al. 2018). Nomenclature and classification follow Ebihara (2018). Light and water requirements are expressed as numbers 1–5, from the lowest requirement (1) to the highest requirement (5).

Order or suborder	Family	Species	Epiphyte (E)/Terrestrial (T)	Light requirement	Water requirement	Diversification age (Myr)
Anatomical and physiological measurement						
Selaginellales	Selaginellaceae	Selaginella moellendorffii	E	4	2	311
Ophioglossales	Ophioglossaceae	Ophioglossum petiolatum	T	4	2	153
Pteridineae	Pteridaceae	Adiantum pedatum	T	3	4	111
Aspleniineae	Thelypteridaceae	Thelypteris dentata	T	3	2	69
Polypodiineae	Dryopteridaceae	Onoclea sensibilis var. interrapta	T	4	4	77
Polypodiineae	Dryopteridaceae	Dryopteris erythrosora	T	2	3	77
Polypodiineae	Davalliaceae	Davallia mariesii	E	3	2	19
Light absorptance measurement						
Salviniales	Marsileaceae	Marsilea quadrifolia	T	5	5	89
Polypodiineae	Polypodiaceae	Pyrrosa lingua	E	4	2	43

pressure deficit, VPD, was 1.0–1.5 kPa, and the flow rate was 500 mL min⁻¹. To obtain light-response curves, the plant leaves were first stabilized for at least 20 min at a CO_2 concentration of 400 μmol mol⁻¹ and PPFD of 200–500 μmol m⁻² s⁻¹. After stabilization, the PPFD was raised to 2,000 μmol m⁻² s⁻¹ to confirm that the stomatal conductance had increased sufficiently, and then the PPFD was lowered stepwise for a total of 11 to 16 points. Each measurement was allowed to stabilize for 5–20 min, where the stomatal conductance was considered stable when it fluctuated within 10%. Maximum stomatal conductance (g_s) was obtained from the maximum light intensity with a PPFD of 2,000 μmol m⁻² s⁻¹. After the measurements were completed, the photosynthetic light-response curve fitting model (Thornley and Johnson 1990) was used to determine the photosynthetic rate at light saturation (P_{max}). Light-saturated PPFD was obtained for each species.

CO_2-response curves (P_N/C_i) were successively obtained for the same leaves used for the light-response curves, just after the measurements of the light-response curves were finished. To obtain P_N/C_i curves, the plant leaves were first stabilized for 30–60 min at a CO_2 concentration of 400 μmol mol⁻¹ until the stomatal conductance change was within 10%. The light intensity for each species was set at the PPFD of light saturation for each species. The CO_2 concentration was changed in the following order: 400, 300, 200, 100, 50, 400, 500, 700; 1,000; 1,500; and 2,000 μmol mol⁻¹. Each measurement was allowed to stabilize for at least 20 min until the stomatal conductance change was within 10%. The maximum carboxylation rate (V_{cmax}) was obtained from P_N/C_i curves (Ethier and Livingston 2004).

Anatomy: For the anatomical measurements of the seven species, light micrographs were obtained for the leaf sections, petiole sections, and the secondary replica of the stomata. The digitized images of the light micrographs were obtained using an optical microscope (*BX51-33*, *Olympus*, Tokyo, Japan) with a digital camera that was attached to the microscope (*U-TVO.5XC*, *Olympus*, Tokyo, Japan). The images were analyzed using *ImageJ* software (Schneider *et al.* 2012).

For the leaf anatomical analyses, sections of 1 × 2 mm were obtained from the central part of the leaves that were used for the leaf gas-exchange measurements ($n = 6$), avoiding the main veins. The leaf sections were fixed in 5% glutaraldehyde in 0.2 M sodium phosphate buffer (pH 7.4) at 4°C, post-fixed in 1% OsO_4 solution at 4°C for 3 h in darkness, dehydrated in a graded ethanol series, and then embedded in Spurr's resin (*Low Viscosity Resin* kit, *TAAB*, Aldermaston, UK). Transverse sections of leaves with 1–3-μm thickness were stained with 1% toluidine blue solution. The mesophyll thickness, chloroplast surface area exposed to intercellular airspaces per leaf area (S_c/S), and mesophyll porosity were measured using digitized images, following previous studies (Hanba *et al.* 2002). For the measurement of S_c/S, the averaged curvature cell correction factor was measured and calculated for the seven species following Thain (1983).

For the measurement of stomatal density, a mixture of silicone (*KE14*, *Shin-Etsu Silicone*, Tokyo) and a catalyst (*CLC-229*, *Shin-Etsu Silicone*, Tokyo) was applied to the lower side of the leaves that were used for the gas-exchange measurements, to make a primary replica. Next, nail varnish was applied to the primary replica to make a secondary replica.

For the analyses of the petiole xylem, the six leaves that photosynthesis was measured from ($n = 6$) were fixed in an FAA solution (formalin: glacial acetic acid: 50% ethanol = 1:1:18). Thereafter, the petiole sections were made by cutting the petiole at 0.5–1 cm from the base into 5–15-μm thin sections using a microtome (*Plant Microtome MT-3*, *Nippon Medical & Chemical Instruments*, Osaka, Japan). The sections were stained with 1% toluidine blue solution. All petiole tracheid lumens were traced. The number of tracheids analyzed was 180–1,000 for each species. The mean tracheid lumen area (T_{area}, μm^2); tracheid density ($T_{density}$, mm^{-2}); the ratio of total tracheid lumen area to petiole cross-sectional area, that is, tracheid lumen fraction (L); and mean tracheid lumen area divided by tracheid density, that is, tracheid composition (N, mm^4), were measured. A large lumen fraction (L) indicates a high fraction of water conduct tissue, and large tracheid composition (N) indicates more large-sized tracheids. We calculated the theoretical hydraulic conductivity per petiole cross-section area, $K_{theoretical}$, following a previous study (Zanne *et al.* 2010):

$$K_{theoretical} = L^{1.5} \, N^{0.5} \tag{1}$$

Measurement of leaf hydraulic properties: The leaf hydraulic property measurements were performed between 9:00–16:00 h, June–October in 2014 and 2015. The leaves used for the measurements were adjacent leaves from the leaves used for the photosynthesis measurements ($n = 6$). To obtain the leaf pressure-volume relationship (PV-curve), the leaves were drained with de-gassed water, sealed with plastic films, and then rehydrated for several hours – overnight to obtain the maximum water content. Thereafter, the leaf water potential was measured stepwise to make PV curves. The leaf water potential at the turgor loss point (Ψ_{tlp}), which is a good indicator for leaf drought tolerance (Bartlett *et al.* 2012, Maréchaux *et al.* 2015), and leaf capacitance, C, were estimated following a previous study (Koide *et al.* 1989). Leaf water potential was measured using a pressure chamber (*Model 600*, *PMS Instrument Company*, OR, USA).

The leaf hydraulic conductance (K_{leaf}) was obtained using the following equation (Brodribb *et al.* 2005):

$$K_{leaf} = C \ln (\Psi_0/\Psi_f)/t \tag{2}$$

where C is the leaf capacitance obtained from PV-curves, and Ψ_0 and Ψ_f are the leaf water potential before rehydration and after rehydration for t seconds, respectively. For the rehydration of the leaves to determine Ψ_0, Ψ_f, and t, the attached leaves were covered with a plastic bag, and then, the leaves were excised in the morning. Thereafter, they were kept in the dark for 20–60 min until the stomata were closed, and all leaves were at the same water potential. After measuring the initial leaf water potential (Ψ_0), the leaf petiole was drained, rehydrated for t seconds, and then the leaf water potential was measured (Ψ_f). The time, t, was about 300 s, until Ψ_f reached half of Ψ_0.

Light absorptance and mesophyll anatomy for two ferns with different mesophyll thickness: The absorptance of radiation was measured using fully expanded, mature leaves in October–November 2019 for two typical fern species that have contrasting mesophyll thickness, *Marsilea quadrifolia* and *Pyrrosia lingua* (Table 1, Fig. 1). The absorptance measurements were repeated in three leaves for *M. quadrifolia* and once for *P. lingua*. The mesophyll anatomical properties, mesophyll thickness, and S_c/S, were measured following the methods described above, using fully matured, expanded leaves ($n = 4$–8).

For the light absorptance measurements, we used a *FieldSpec 3* spectroradiometer (*Analytical Spectral Devices*, Boulder, CO, USA) and an *LI-1800* integrating sphere (*Li-Cor*, Lincoln, NE, USA). Since the target fern leaves were too narrow to cover the sample port of the integrating sphere fully, we adopted a leaf array method to measure the reflectance and transmittance (Noda *et al.* 2013, Hanba *et al.* 2023). We calculated the reflectance from the leaf array (ρ_a) and transmittance of the leaf array from the illuminated side (τ_a) as follows:

$$\rho_a = \frac{F_{ar} - F_{vr}}{F_{aw} - F_{vr}} \rho_w \frac{1}{1 - G_r} \tag{3}$$

$$\tau_a = \left(\frac{F_{at}}{F_{aw} - F_{vr}} \rho_w - G_t \rho_c \right) \frac{1}{1 - G_t} \tag{4}$$

where ρ_w and ρ_c is the reflectance of the $BaSO_4$ reference surface and the cavity cell wall, respectively. F_{vr} is the flux of stray light measured in reflectance mode with a vacant sample port. F_{ar}, F_{aw}, and F_{at} are flux from the leaf array in reflectance mode, in white reference mode, and in transmittance mode, respectively. G_r and G_t are the gap fraction at 400 nm in reflectance mode and transmittance mode, respectively. We calculated leaf absorptance using the following equation:

$$\text{Absorptance} = 1 - \text{reflectance} - \text{transmittance} \tag{5}$$

We focused on the absorption spectrum from 350 to 699 nm, because it covers the absorption spectrum of the main pigments, such as chlorophyll (Chl) *a*, Chl *b*, and flavonols, in the leaves considering the blue shift of the absorbance spectrum measured *in vitro* (Solovchenko 2010, Kume *et al.* 2018).

Comparison between ferns and bryophytes using datasets from previous studies: The mean values for mesophyll thickness, S_c/S, P_{max}, S_c/S on a mesophyll-thickness-basis, and $P_{max}/(S_c/S)$ were obtained for ferns and bryophytes. To make comparisons between different traits, the values were normalized using the mean and standard deviation of each trait. For the ferns, data from previous studies (Zhang *et al.* 2014, Nishida *et al.* 2015, Tosens

et al. 2016) and those of the present study were pooled. For the bryophytes, data from previous studies (Takemura *et al.* 2017, Carriquí *et al.* 2019, Perera-Castro *et al.* 2022) were used. In total, 69 species of ferns and 23 species of bryophytes were used for the analyses.

Statistical analysis: For the traits of leaf anatomy, leaf gas exchange, petiole xylem anatomy, and leaf hydraulics for the seven fern species, we performed a one-way analysis of variance (*ANOVA*) to test the species' effect on these traits. We focused on 12 traits: (*1*) mesophyll thickness, (*2*) S_c/S, and (*3*) mesophyll porosity as the leaf anatomical traits, (*4*) P_{max}, (*5*) g_s, and (*6*) V_{cmax} as the leaf gas exchange traits, (*7*) tracheid area (T_{area}), (*8*) tracheid density ($T_{density}$), and (*9*) theoretical hydraulic conductivity ($K_{theoretical}$) as the petiole xylem anatomical traits, and (*10*) stomatal density, (*11*) leaf water potential at the turgor loss point (Ψ_{tlp}), and (*12*) leaf hydraulic conductivity (K_{leaf}) as the leaf hydraulic traits.

The correlations among these traits were analyzed using *Pearson*'s product-moment correlation coefficient. The relationships between the two traits were analyzed using linear regression. The comparisons between the two mean values were conducted using *Welch*'s *t*-test. Factor analysis was performed for the seven traits, mesophyll-thickness-based P_{max}, g_s, S_c/S and $K_{theoretical}$, S_c/S-based P_{max} [$P_{max}/(S_c/S)$], mesophyll thickness, and leaf water potential at the turgor loss point ($-\psi_{tlp}$). The comparison between ferns and bryophytes was performed using *Mann-Whitney*'s *U*-test. These statistical analyses were performed using *EZR* (Kanda 2013) and *Rcmdr* (*ver. 2.7–2*) for *R* software, *R ver. 4.2.1* (*R Core Team 2022*).

Results

Variations in mesophyll traits in the seven fern species: The leaf mesophyll anatomy and xylem anatomy of the leaf petioles varied significantly between species (Fig. 1*A,C*). *S. moellendorffii* and *A. pedatum* had a thin leaf mesophyll with a primitive type of stele, protostele, that is composed of a solid core of xylem mass surrounded by phloem. The other five species had a thicker leaf mesophyll with more developed mesophyll cell layers. Their stele type was siphonostele. In all the fern species, the palisade and spongy cells were not distinguishable.

The differences between species were significant in all 12 traits (Fig. 2). The leaf mesophyll thickness varied 9.2-fold, whereas the variations in S_c/S and mesophyll porosity were much smaller, 1.9–2.7-fold (Fig. 2*A*). The variations in the three leaf gas-exchange traits, P_{max}, g_s, and V_{cmax}, were similarly much smaller than those in mesophyll thickness, 2.3–3.2-fold (Fig. 2*B*). On the other hand, the variations in the xylem anatomical traits in the leaf petiole, T_{area}, $T_{density}$, and $K_{theoretial}$, were large, 6.5–9.4-fold (Fig. 2*C*). Similarly, the variations in the leaf hydraulic traits, stomatal density, and K_{leaf}, were large, 5.9–7.5-fold (Fig. 2*D*). ψ_{tlp} varied from –1.7 to –0.8 MPa (Fig. 2*D*).

Correlations among traits in the seven fern species: The correlation matrix showed that mesophyll thickness positively correlated to the mesophyll trait S_c/S and the

gas-exchange trait V_{cmax} (Fig. 3*A*; Table 1S, *supplement*). In contrast, mesophyll thickness negatively correlated to the xylem anatomical traits and leaf hydraulic traits T_{area} and $K_{theoretical}$, stomatal density, and Ψ_{tlp}. S_c/S was positively correlated to the gas-exchange traits P_{max} and V_{cmax}, and these two gas-exchange traits strongly correlated with each other. For the xylem anatomical and leaf hydraulic traits, strong relationships were obtained between T_{area} and $K_{theoretical}$, as well as among stomatal density, Ψ_{tlp}, and K_{leaf}.

When the area-based mesophyll anatomical traits, such as S_c/S, and leaf gas-exchange traits, such as P_{max}, are expressed on a mesophyll-thickness-basis, we can obtain the leaf-volume-based traits (Fig. 3*B–E*). Mesophyll-thickness-based S_c/S was positively correlated to the inverse of mesophyll thickness (Fig. 3*B*). Mesophyll-thickness-based S_c/S and mesophyll-thickness-based P_{max} were positively correlated (Fig. 3*C*). On the other hand, the ratio of P_{max} to S_c/S, $P_{max}/(S_c/S)$, that is, photosynthetic rate per chloroplast surface area, was almost constant against the changes in mesophyll thickness (Fig. 3*D*).

Factor analysis revealed that factor 1 explained 51.5% of the variation, in which factor 1 related to light capture, CO_2 diffusion, and leaf water transport on a mesophyll-thickness-basis (Fig. 3*E*). A thick mesophyll, which had a negative loading on the factor 1 axis, involved a smaller surface area of chloroplasts (S_c/S), photosynthesis (P_{max}), stomatal conductance (g_s), and theoretical leaf hydraulic conductivity ($K_{theoretical}$) on a mesophyll-thickness-basis, which had positive loadings on the factor 1 axis. The negative loading of $-\Psi_{tlp}$ on the factor1 axis were obtained. The factor 2 axis, which explained 15.6% of the variation, was related to $P_{max}/(S_c/S)$.

Light absorptance in the two fern species: The mesophyll thickness and S_c/S of *Pyrrosia lingua* were significantly larger than those of *Marsilea quadrifolia* (Fig. 4*A,B*; *p*<0.001). The light absorptance of 450–700 nm was larger in *P. lingua* than that in *M. quadrifolia* (Fig. 4*B*, *p*<0.001). The absorptance, both mesophyll-thickness-based and S_c/S-based, was larger in *M. quadrifolia* than those in *P. lingua*, in which the difference between species was less in the S_c/S-based absorptance than that in mesophyll-thickness-based absorptance (Fig. 4*C*).

Comparison of the traits between ferns and bryophytes: When the normalized mean values for mesophyll thickness, S_c/S, P_{max}, S_c/S on a mesophyll-thickness-basis, and $P_{max}/(S_c/S)$ were compared between ferns and bryophytes using data obtained in previous studies, ferns had larger values than those of bryophytes, except for S_c/S on a mesophyll-thickness-basis (Fig. 5, *p*<0.01). Bryophytes had larger S_c/S on a mesophyll-thickness-basis than that of ferns (*p*<0.1).

Discussion

The positive relationship between mesophyll thickness and S_c/S (Fig. 3*A*) shows that the ferns with a thick mesophyll have many chloroplasts per unit leaf area. An increase in S_c/S with an increase in mesophyll thickness
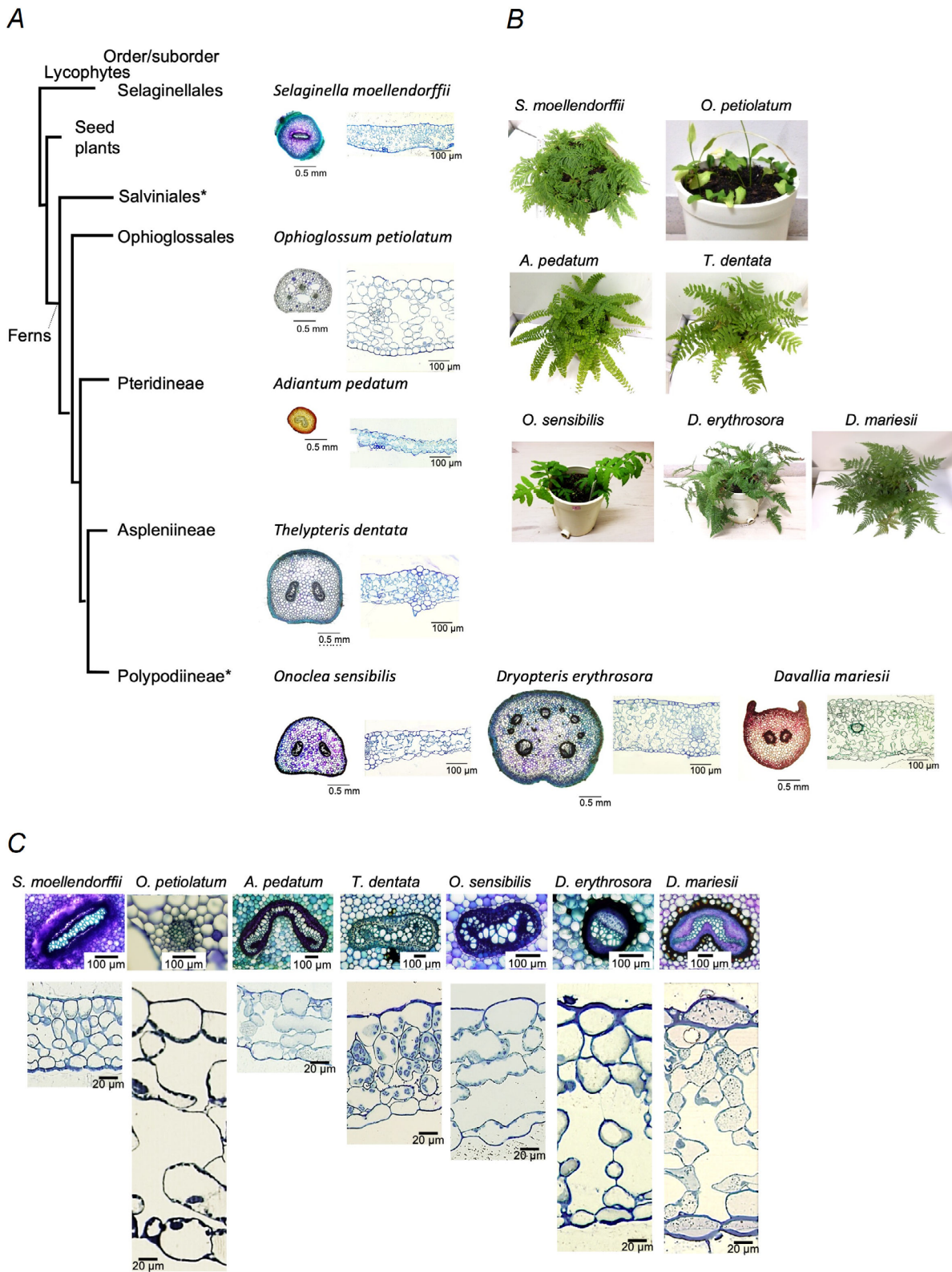
Fig. 1. (*A*) Phylogeny tree of the seven fern species that were used for the measurements of the mesophyll and xylem anatomy, leaf gas exchange, and leaf hydraulics. The images of the petioles and leaf sections are shown for each species. (*B*) Plant images of the ferns used in the present study. (*C*) Enlarged images of the petiole xylem and leaf sections for each species. *Asterisks* (*) mean that the two additional species of these orders, *Marsilea quadrifolia* (Salviniales) and *Pyrrosa lingua* (Polypodiineae), were used for the light absorptance measurement.
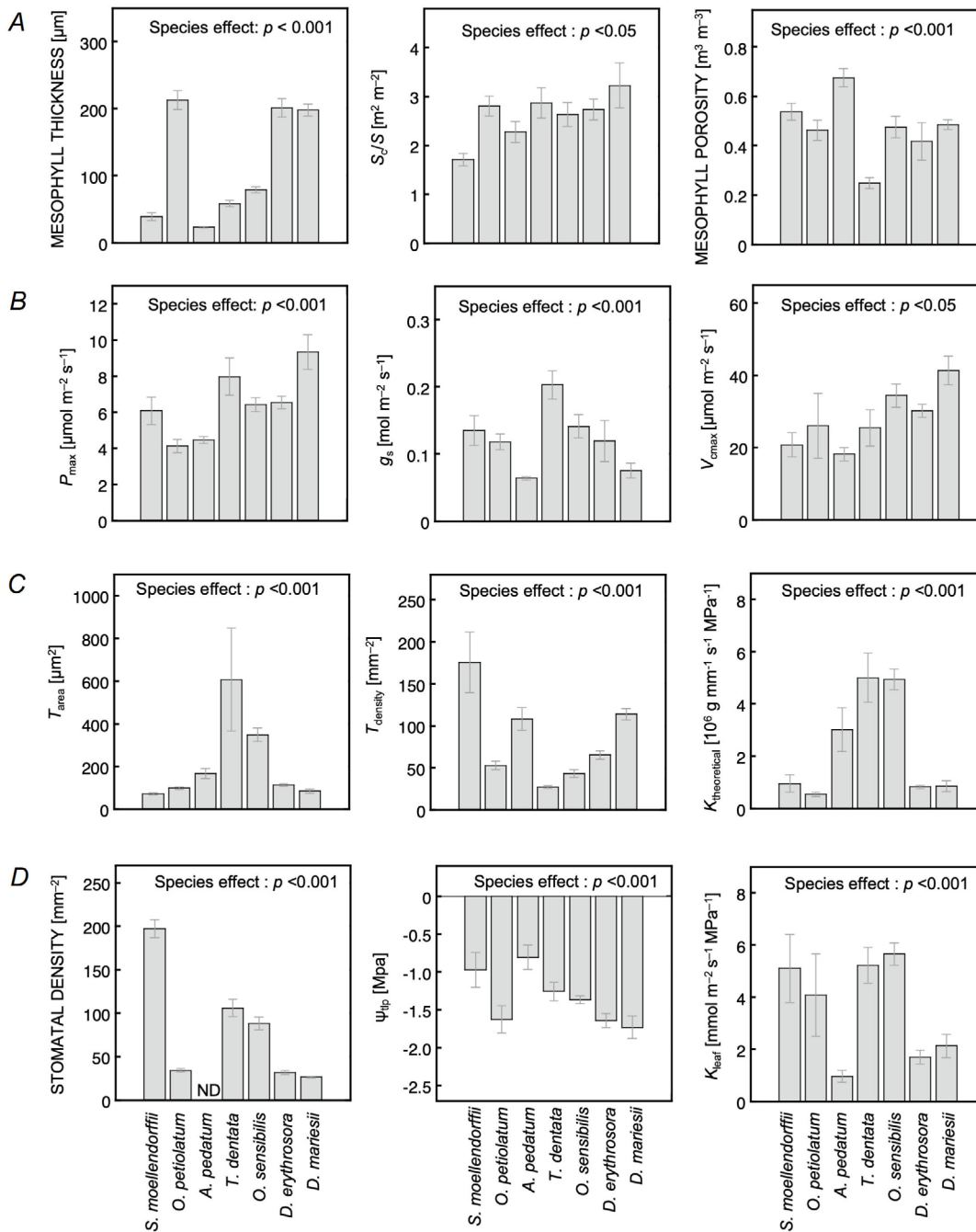
Fig. 2. Mean values of the twelve leaf traits for the seven fern species ($n = 6$). *Bars* represent standard errors. (*A*) Mesophyll anatomical traits, mesophyll thickness, S_c/S, and mesophyll porosity; (*B*) leaf gas-exchange traits, P_{max}, g_s, and V_{cmax}; (*C*) petiole xylem anatomical traits, tracheid area (T_{area}), tracheid density ($T_{density}$), and theoretical hydraulic conductivity ($K_{theorecital}$); and (*D*) leaf hydraulic traits, stomatal density, leaf water potential at the turgor loss point (ψ_{tlp}), and leaf hydraulic conductivity (K_{leaf}). No data were obtained for the stomatal density of *Adiantum pedatum*. The species effect on each trait was tested by one-way *ANOVA*; the *P*-values are shown.

has been reported for sun and shade leaves (Hanba *et al.* 2002, Oguchi *et al.* 2005, Tosens *et al.* 2012, Fini *et al.* 2016), as well as for leaves with different developmental stages (Tosens *et al.* 2012). The thick mesophyll with a large number of chloroplasts allows the ferns to absorb much light (Fig. 4*A,B*), as well as to enhance CO_2 diffusion within the leaves (Terashima *et al.* 2011, Mizokami *et al.* 2022), which should enhance the leaf-area-based photosynthetic efficiency. Actually, S_c/S imposes a positive effect on both P_{max} and V_{cmax} (Fig. 3*A*), which confirms the results of previous studies on fern species (Tosens *et al.* 2016, Carriquí *et al.* 2019).
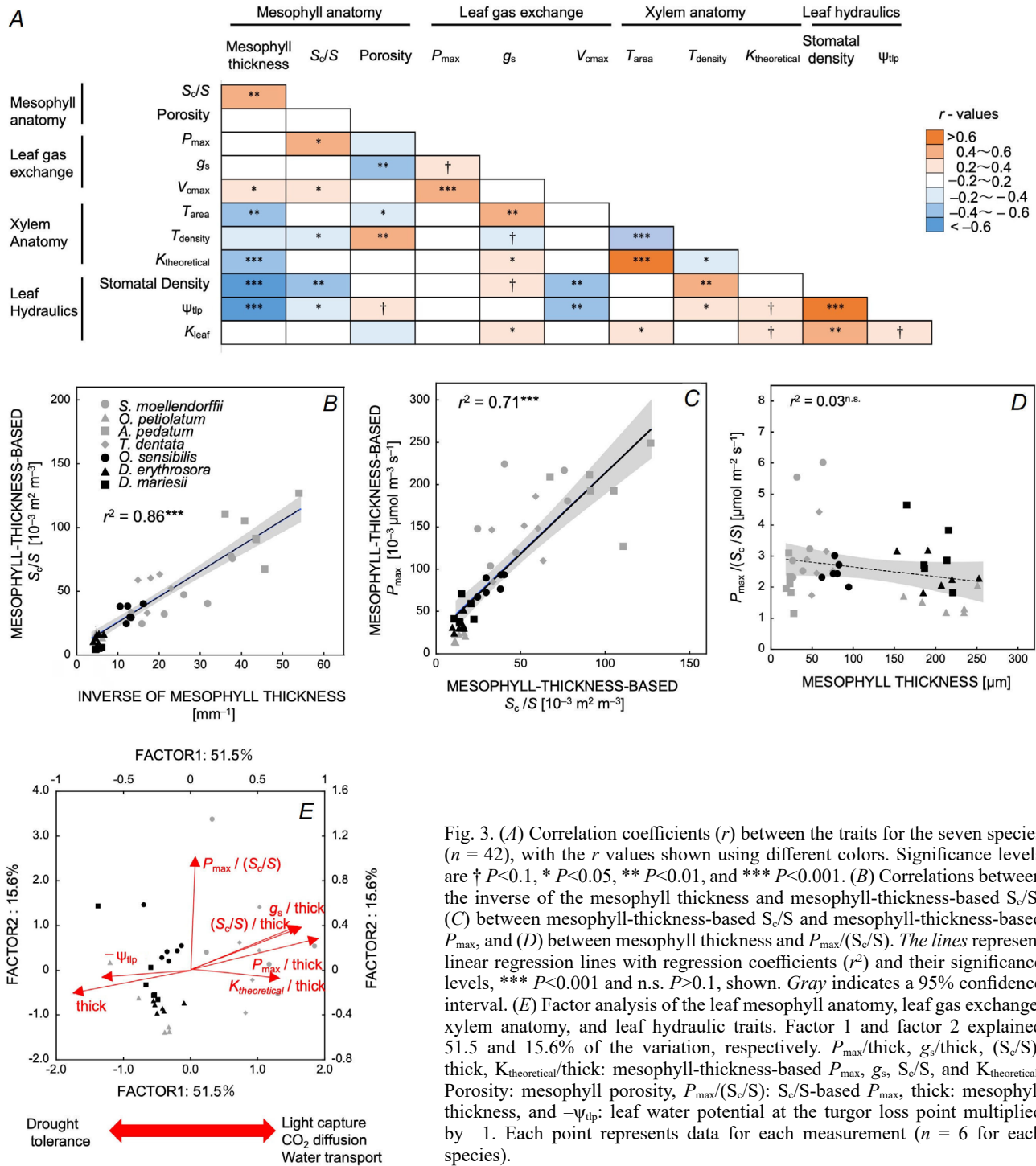
Fig. 3. (*A*) Correlation coefficients (*r*) between the traits for the seven species (*n* = 42), with the *r* values shown using different colors. Significance levels are † *P*<0.1, * *P*<0.05, ** *P*<0.01, and *** *P*<0.001. (*B*) Correlations between the inverse of the mesophyll thickness and mesophyll-thickness-based S_c/S, (*C*) between mesophyll-thickness-based S_c/S and mesophyll-thickness-based P_{max}, and (*D*) between mesophyll thickness and $P_{max}/(S_c/S)$. *The lines* represent linear regression lines with regression coefficients (*r²*) and their significance levels, *** *P*<0.001 and n.s. *P*>0.1, shown. *Gray* indicates a 95% confidence interval. (*E*) Factor analysis of the leaf mesophyll anatomy, leaf gas exchange, xylem anatomy, and leaf hydraulic traits. Factor 1 and factor 2 explained 51.5 and 15.6% of the variation, respectively. P_{max}/thick, g_s/thick, (S_c/S)/thick, $K_{theoretical}$/thick: mesophyll-thickness-based P_{max}, g_s, S_c/S, and $K_{theoretical}$. Porosity: mesophyll porosity, $P_{max}/(S_c/S)$: S_c/S-based P_{max}, thick: mesophyll thickness, and $-\psi_{tlp}$: leaf water potential at the turgor loss point multiplied by –1. Each point represents data for each measurement (*n* = 6 for each species).

On the other hand, mesophyll thickness is negatively correlated to the xylem anatomical traits and leaf hydraulic traits that are related to water transport, such as tracheid area (Pittermann *et al.* 2011) and stomatal density (Zhang *et al.* 2014), involving a negative correlation between mesophyll thickness and theoretical hydraulic conductivity (Fig. 3*A*). Additionally, the negative relationship between ψ_{tlp} and mesophyll thickness (Fig. 3*A*)

indicates that species with a large mesophyll thickness have high drought tolerance (Bartlett *et al.* 2012, Maréchaux *et al.* 2015). These results suggest that ferns with a large mesophyll thickness, having a high ability of light capture and CO$_2$ uptake on a leaf-area-basis, have high drought tolerance at the expense of leaf water conductivity. This supports a previous study (Brodribb *et al.* 2007). This result highlights the tight coordination between mesophyll
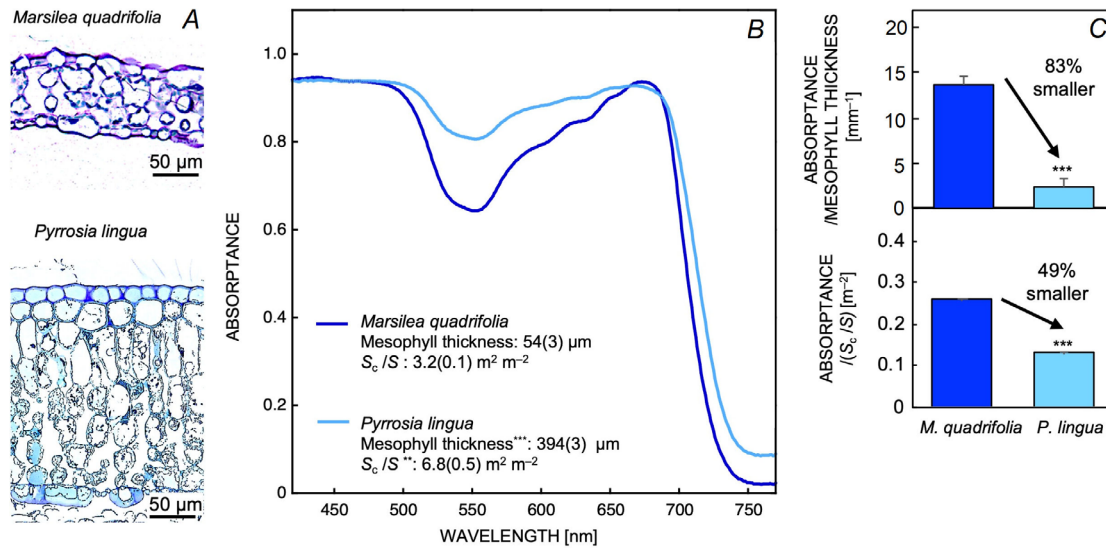
Fig. 4. (*A*) Light micrographs of the leaf sections of the two fern species, *Marsilea quadrifolia* and *Pyrrosa lingua*. (*B*) Absorptance spectra of the leaves of *M. quadrifolia* and *P. lingua*. The data for three leaves were pooled for *M. quadrifolia* and then mean values were calculated. For *P. lingua*, the data were obtained from a single leaf. Mean (standard error, SE) values of mesophyll thickness and S_c/S are shown for each species ($n = 4$–8), tested by *Welch*'s *t*-test, with significance levels of ** $P<0.01$ and *** $P<0.001$. (*C*) Mean absorptance of 450–700 nm on a mesophyll-thickness-basis and S_c/S-basis. The differences between species were tested using *Welch*'s *t*-test, with a significance level of *** $P<0.001$.
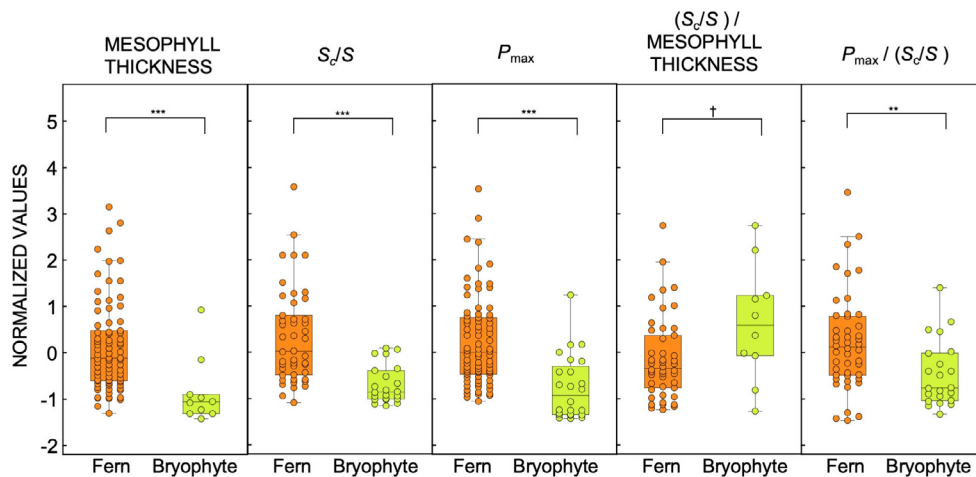

Fig. 5. Box plots are shown for the mesophyll anatomical traits and gas-exchange traits for the ferns ($n = 46$–78) and bryophytes ($n = 10$–24). The data for ferns were pooled from the present study and previous studies (Zhang *et al.* 2014, Nishida *et al.* 2015, Tosens *et al.* 2016), and the data for bryophytes were obtained from previous studies (Takemura *et al.* 2017, Carriquí *et al.* 2019, Perera-Castro *et al.* 2022). The data were normalized using the mean and standard deviation for each trait, and then the mean normalized values were compared between ferns and bryophytes using *Mann Whitney*'s *U*-test, with significance levels of † $P<0.1$, ** $P<0.01$, and *** $P<0.001$. The data include 23 species of bryophytes and 69 species of ferns, with which some of the species have multiple data. The numbers of data values depend on the variables, where $n = 10$–14 for bryophytes and $n = 46$–78 for ferns. Each point represents a data value.

thickness and leaf hydraulic properties, which has been little studied in ferns. Previous studies on epiphytes and terrestrial ferns reported that epiphyte ferns, which are more susceptible to drought stress, have lower hydraulic conductivity (Watkins *et al.* 2010, Campany *et al.* 2021).

A thick mesophyll with many chloroplasts is advantageous for photosynthesis in a strong light environment (Oguchi *et al.* 2005) because even the chloroplasts that

are located on the deeper side of the leaves can absorb enough light. However, many fern species inhabit light-limited conditions (Royo and Carson 2006), where a high efficiency of light capture per chloroplast is essential for effective photosynthesis. The lack of palisade tissue in fern species (Fig. 1*C*) increases the amount of light received per chloroplast (Kume 2017). Additionally, a lower density of chloroplasts in thick leaves allows the light

to spread to the depths of the leaf, which enhances the availability of the scattered light within a leaf (Terashima *et al.* 2009). When S_c/S is expressed on a mesophyll-thickness-basis, it is inversely proportional to mesophyll thickness (Fig. 3*B*), which indicates that fern species decrease chloroplast density with an increase in mesophyll thickness. A decrease in chloroplast density was observed in the images of leaf sections, where the three fern species with a large mesophyll thickness, *S. moellendorffii*, *D. erythrosora*, and *D. mariesii*, have large gaps between the chloroplasts in the mesophyll cells (Fig. 1*C*). As a result of such a reduction in chloroplast density, light absorptance per chloroplast, *i.e.*, light absorptance per S_c/S, can be less reduced in the species with a thick mesophyll (Fig. 4*B*). Such a high efficiency of light capture per chloroplast supports the findings of a previous study that found increases in the light absorptance per chlorophyll in the shade leaves of a temperate deciduous tree (Baltzer and Thomas 2005). These suggest that among the plant groups, ferns, and trees (angiosperms) can increase light absorptance per chloroplast by adjusting the chloroplast density in the leaves. The almost constant photosynthetic rate per chloroplast surface area, $P_{max}/(S_c/S)$, against mesophyll thickness in the fern species (Fig. 3*D*) may partly benefit from such enhancement of light capture by each chloroplast *via* regulation of the chloroplast density and mesophyll development.

On the other hand, on a mesophyll-thickness-basis, the decrease in S_c/S, *i.e.*, the decrease in chloroplast density, causes a reduction in photosynthesis (Fig. 3*C*). This result supports a previous study that reported reductions in the chloroplast density and photosynthesis on a mesophyll-thickness-basis in potassium (K)-deficient plants (Hu *et al.* 2020). Factor analysis reveals that photosynthesis on a mesophyll-thickness-basis strongly coordinates with mesophyll-thickness-based anatomical and physiological traits, which suggests strong links among leaf-volume-based light capture, CO_2 diffusion, and water transport for leaf photosynthesis (Fig. 3*E*).

The slightly lower mesophyll-thickness-based S_c/S in ferns than those in bryophytes (Fig. 5, $p<0.1$) suggests that ferns can increase light capture more efficiently by reducing the chloroplast density in coordination with an increase in leaf mesophyll thickness. The higher $P_{max}/(S_c/S)$ of the ferns than those of bryophytes (Fig. 5, $p<0.01$) may partly benefit from such enhancement of light capture by each chloroplast *via* regulation of the chloroplast density. Previous studies reported a much lower photosynthetic rate in bryophytes than in ferns, largely due to lower CO_2 diffusional conductance in bryophytes (Gago *et al.* 2019). Our present result suggests that the lower photosynthetic rate in bryophytes (Fig. 5, $p<0.001$) may be partly affected by the low ability to capture light due to the low ability to adjust chloroplast density.

In conclusion, the difference in mesophyll thickness between fern species is closely linked to leaf-area-based gas exchange, xylem anatomy, and leaf hydraulic capacity. On a leaf-area-basis, fern species with a large mesophyll thickness have a high photosynthetic capacity (V_{cmax}) that is supported by the large light capture, which is accompanied by higher drought tolerance and lower leaf hydraulic conductance. The reduction in chloroplast density with the increase in mesophyll thickness may partly compensate for the reduction in photosynthetic rate by improving the optical properties within the mesophyll tissue. The higher photosynthetic rate per chloroplast in ferns than in bryophytes is shown in the present study for the first time, which suggests evolutional changes in the ability of light capture and its effect on photosynthesis. In the present study, it is difficult to analyze the effect of chloroplast adjustment on light capture in detail because our measurements of leaf optical properties were limited to only two species. Further studies will be needed to clarify the effect of chloroplast adjustment on leaf gas exchange and leaf hydraulic properties *via* the measurement of leaf light absorptance.

References

Aasamaa K., Sõber A., Rahi M.: Leaf anatomical characteristics associated with shoot hydraulic conductance, stomatal conductance and stomatal sensitivity to changes of leaf water status in temperate deciduous trees. – Funct. Plant Biol. **28**: 765-774, 2001.

Baltzer J.L., Thomas S.C.: Leaf optical responses to light and soil nutrient availability in temperate deciduous trees. – Am. J. Bot. **92**: 214-223, 2005.

Bartlett M.K., Scoffoni C., Sack L.: The determinants of leaf turgor loss point and prediction of drought tolerance of species and biomes: a global meta-analysis. – Ecol. Lett. **15**: 393-405, 2012.

Brodribb T.J., Feild T.S., Jordan G.J.: Leaf maximum photosynthetic rate and venation are linked by hydraulics. – Plant Physiol. **144**: 1890-1898, 2007.

Brodribb T.J., Holbrook N.M., Zwieniecki M.A., Palma B.: Leaf hydraulic capacity in ferns, conifers and angiosperms: Impacts on photosynthetic maxima. – New Phytol. **165**: 839-846, 2005.

Campany C.E., Pittermann J., Baer A. *et al.*: Leaf water relations in epiphytic ferns are driven by drought avoidance rather than tolerance mechanisms. – Plant Cell Environ. **44**: 1741-1755, 2021.

Carriquí M., Roig-Oliver M., Brodribb T.J. *et al.*: Anatomical constraints to nonstomatal diffusion conductance and photosynthesis in lycophytes and bryophytes. – New Phytol. 222: 1256-1270, 2019.

Cui M., Vogelmann T.C., Smith W.K.: Chlorophyll and light gradients in sun and shade leaves of *Spinacia oleracea*. – Plant Cell Environ. **14**: 493-500, 1991.

Ebihara A.: [The Standard of Ferns and Lycophytes in Japan.] Gakken Plus, Tokyo 2018. [In Japanese]

Ethier G.J., Livingston N.J.: On the need to incorporate sensitivity to CO_2 transfer conductance into the Farquhar–von Caemmerer–Berry leaf photosynthesis model. – Plant Cell Environ. **27**: 137-153, 2004.

Fini A., Loreto F., Tattini M. *et al.*: Mesophyll conductance plays a central role in leaf functioning of Oleaceae species exposed to contrasting sunlight irradiance. – Physiol. Plantarum **157**: 54-68, 2016.

Gago J., Carriquí M., Nadal M. *et al.*: Photosynthesis optimized across land plant phylogeny. – Trends Plant Sci. **24**: 947-958, 2019.

Hanba Y.T., Kogami H., Terashima I.: The effect of growth irradiance on leaf anatomy and photosynthesis in *Acer* species

differing in light demand. – Plant Cell Environ. **25**: 1021-1030, 2002.

Hanba Y.T., Miyazawa S.-I., Terashima I.: The influence of leaf thickness on the CO_2 transfer conductance and leaf stable carbon isotope ratio for some evergreen tree species in Japanese warm-temperate forests. – Funct. Ecol. **13**: 632-639, 1999.

Hanba Y.T., Nishida K., Tsutsui Y. *et al.*: Leaf optical properties and photosynthesis of fern species with wide range of divergence time in relation to the mesophyll anatomy. – Ann. Bot.-London **131**: 437-450, 2023.

Hu W., Lu Z., Meng F. *et al.*: The reduction in leaf area precedes that in photosynthesis under potassium deficiency: the importance of leaf anatomy. – New Phytol. **227**: 1749-1763, 2020.

Kanda Y.: Investigation of the freely available easy-to-use software 'EZR' for medical statistics. – Bone Marrow Transplant. **48**: 452-458, 2013.

Koide R.T., Robichaux R.H., Morse S.R., Smith C.M.: Plant water status, hydraulic resistance and capacitance. – In: Pearcy R.W., Ehleringer J.R., Mooney H.A., Rundel P.W. (ed.): Plant Physiological Ecology. Pp. 161-183. Springer, Dordrecht 1989.

Kume A., Akitsu T., Nasahara K.N.: Why is chlorophyll *b* only used in light-harvesting systems? – J. Plant Res. **131**: 961-972, 2018.

Kume A.: Importance of the green color, absorption gradient, and spectral absorption of chloroplasts for the radiative energy balance of leaves. – J. Plant Res. **130**: 501-514, 2017.

Lambers H., Oliveira R.S.: Plant Physiological Ecology. Pp. 736. Springer, Cham 2019.

Maréchaux I., Bartlett M.K., Sack L. *et al.*: Drought tolerance as predicted by leaf water potential at turgor loss point varies strongly across species within an Amazonian forest. – Funct. Ecol. **29**: 1268-1277, 2015.

Matos F.S., Wolfgramm R., Gonçalves F.V. *et al.*: Phenotypic plasticity in response to light in the coffee tree. – Environ. Exp. Bot. **67**: 421-427, 2009.

Mizokami Y., Oguchi R., Sugiura D. *et al.*: Cost-benefit analysis of mesophyll conductance: diversities of anatomical, biochemical and environmental determinants. – Ann. Bot.-London **130**: 265-283, 2022.

Nishida K., Kodama N., Yonemura S., Hanba Y.T.: Rapid response of leaf photosynthesis in two fern species *Pteridium aquilinum* and *Thelypteris dentata* to changes in CO_2 measured by tunable diode laser absorption spectroscopy. – J. Plant Res. **128**: 777-789, 2015.

Noda H.M., Motohka T., Murakami K. *et al.*: Accurate measurement of optical properties of narrow leaves and conifer needles with a typical integrating sphere and spectroradiometer. – Plant Cell Environ. **36**: 1903-1909, 2013.

Oguchi R., Hikosaka K., Hirose T.: Leaf anatomy as a constraint for photosynthetic acclimation: Differential responses in leaf anatomy to increasing growth irradiance among three deciduous trees. – Plant Cell Environ. **28**: 916-927, 2005.

Perera-Castro A.V., Waterman M.J., Robinson S.A., Flexas J.: Limitations to photosynthesis in bryophytes: certainties and uncertainties regarding methodology. – J. Exp. Bot. **73**: 4592-4604, 2022.

Pittermann J., Limm E., Rico C., Christman M.A.: Structure–function constraints of tracheid-based xylem: a comparison of conifers and ferns. – New Phytol. **192**: 449-461, 2011.

Pryer K.M., Schuettpelz E., Wolf P.G. *et al.*: Phylogeny and evolution of ferns (monilophytes) with a focus on the early leptosporangiate divergences. – Am. J. Bot. **91**: 1582-1598, 2004.

R Core Team: *R*: A language and environment for statistical computing. R Foundation for Statistical Computing, Vienna, Austria. *Available at*: https://www.R-project.org/, 2022.

Ren T., Weraduwage S.M., Sharkey T.D.: Prospects for enhancing leaf photosynthetic capacity by manipulating mesophyll cell morphology. – J. Exp. Bot. **70**: 1153-1165, 2019.

Royo A.A., Carson W.P.: On the formation of dense understory layers in forests worldwide: consequences and implications for forest dynamics, biodiversity, and succession. – Can. J. Forest Res. **36**: 1345-1362, 2006.

Sack L., Scoffoni C., John G.P. *et al.*: How do leaf veins influence the worldwide leaf economic spectrum? Review and synthesis. – J. Exp. Bot. **64**: 4053-4080, 2013.

Sack L., Scoffoni C., Johnson D.M. *et al.*: The anatomical determinants of leaf hydraulic function. – In: Hacke U. (ed.): Functional and Ecological Xylem Anatomy. Pp. 255-271. Springer, Cham 2015.

Schneider C.A., Rasband W.S., Eliceiri K.W.: NIH Image to ImageJ: 25 years of image analysis. – Nat. Methods **9**: 671-675, 2012.

Schuettpelz E., Pryer K.M.: Evidence for a Cenozoic radiation of ferns in an angiosperm-dominated canopy. – PNAS **106**: 11200-11205, 2009.

Solovchenko A.: Screening pigments: General questions. – In: Photoprotection in Plants. Springer Series in Biophysics. Vol. 14. Pp. 9-31. Springer, Berlin-Heidelberg 2010.

Takemura K., Kamachi H., Kume A. *et al.*: A hypergravity environment increases chloroplast sizes, photosynthesis and plant growth of the moss *Physcomitrella patens*. – J. Plant Res. **130**: 181-192, 2017.

Terashima I., Fujita T., Inoue T. *et al.*: Green light drives leaf photosynthesis more efficiently than red light in strong white light: Revisiting the enigmatic question of why leaves are green. – Plant Cell Physiol. **50**: 684-697, 2009.

Terashima I., Hanba Y.T., Tholen D., Niinemets Ü.: Leaf functional anatomy in relation to photosynthesis. – Plant Physiol. **155**: 108-116, 2011.

Testo W., Field A., Barrington D.: Overcoming among-lineage rate heterogeneity to infer the divergence times and biogeography of the clubmoss family Lycopodiaceae. – J. Biogeogr. **45**: 1929-1941, 2018.

Thain J.F.: Curvature correction factors in the measurement of cell surface areas in plant tissues. – J. Exp. Bot. **34**: 87-94, 1983.

Thornley J.H.M., Johnson I.R.: Plant and Crop Modelling: A Mathematical Approach to Plant and Crop Physiology. Pp. 669. The Blackburn Press, New Jersey 1990.

Tosens T., Niinemets Ü., Vislap V. *et al.*: Developmental changes in mesophyll diffusion conductance and photosynthetic capacity under different light and water availabilities in *Populus tremula*: how structure constrains function. – Plant Cell Environ. **35**: 839-856, 2012.

Tosens T., Nishida K., Gago J. *et al.*: The photosynthetic capacity in 35 ferns and fern allies: mesophyll CO_2 diffusion as a key trait. – New Phytol. **209**: 1576-1590, 2016.

Watkins J.E., Holbrook N.M., Zwieniecki M.A.: Hydraulic properties of fern sporophytes: consequences for ecological and evolutionary diversification. – Am. J. Bot. **97**: 2007-2019, 2010.

Zanne A.E., Westoby M., Falster D.S. *et al.*: Angiosperm wood structure: Global patterns in vessel anatomy and their relation to wood density and potential conductivity. – Am. J. Bot. **97**: 207-215, 2010.

Zhang S.-B., Sun M., Cao K.-F. *et al.*: Leaf photosynthetic rate of tropical ferns is evolutionarily linked to water transport capacity. – PLoS ONE **9**: e84682, 2014.